Hausmannite and braunite nodules from the Aracena area (Iberian Massif, SW Spain)

Juan Jiménez-Millán

Departamento de Geología,
Universidad de Jaén,
Facultad de Ciencias Experimentales,
Campus Universitario, 23071 Jaén,
Spain

Nicolás Velilla

Departamento de Mineralogía y Petrología,
Universidad de Granada,
Facultad de Ciencias,
Fuentenueva s/n, 18002 Granada,
Spain

BRAUNITE and hausmannite are two of the most common oxides containing Mn^{3+}. Minerals of the braunite group include braunite I ($Mn^{2+}Mn_6^{3+}SiO_{12}$), which presents a structure defined by alternation of layers of $[Mn^{3+}O_6]$ octahedra, $[SiO_4]$ tetrahedra, and $[Mn^{2+}O_8]$ polyhedra (de Villiers, 1975); braunite II ($CaMn_{14}^{3+}SiO_{24}$, de Villiers and Herbstein, 1967) and neltnerite ($CaMn_6^{3+}SiO_{12}$). Hausmannite is the Mn-rich end-member of the Fe_3O_4–Mn_3O_4 system. The structure of hausmannite is tetragonal but analogous to that of Fe_3O_4 spinel. Occurrences of braunite and hausmannite have been reported in a wide variety of geological environments (see Huebner, 1976; Robie *et al.*, 1995). This study presents a geochemical characterization of braunite and hausmannite nodules associated with carbonate and volcanic rocks in order to deduce their origin.

Geological context

The studied rocks belong to the southernmost band of the Ossa-Morena Zone in the Southern Iberian Massif, known as the Evora-Beja-Aracena massif. The Mn-rocks of the Aracena area occur in the northern unit of this massif, whose metamorphic grade corresponds to greenschist facies. The stratigraphic sequence is volcano-sedimentary in character, consisting of metatuffs, metabasites, metacinerites, and carbonate rocks. A small diorite intrusion crops out a few metres from the studied rocks, developing a narrow aureole of thermal metamorphism.

Petrography and geochemistry

The petrographic study was carried out using X-ray diffraction (Siemens D5000), polarizing microscope, and a Camebax SX-50 automated electron microprobe in wavelength-dispersive mode under the following conditions: accelerating voltage 20 kV; probe current 5 nA; electron beam diameter 0.5 μm. The following compounds were used as standards: albite, orthoclase, periclase, wollastonite and synthetic oxides (Al_2O_3, Fe_2O_3 and $MnTiO_3$). Whole-rock analyses were carried out by X-ray fluorescence for major elements, and neutron activation and ICP for minor elements.

Hausmannite occurs as centimetre-sized nodules without internal structure in rocks containing spessartine bands, rhodonite, Mn-phlogopite, and manganoan calcite. Hausmannite is never in direct contact with spessartine or rhodonite since a reaction band of tephroite always appears between them (Fig. 1A). Hausmannite is massive with a deep-red colour in transmitted light. Deep-red internal reflections and distinct anisotropy are observed in reflected light. The hausmannite microanalyses (Table 1) reveal that their chemical composition is close to the $Mn^{2+}Mn_2^{3+}O_4$ end-member (around 90%). Significant Fe_2O_3 contents were detected. Thus, the values of the $Mn^{2+}Fe_2^{3+}O_4$ end-member are around 10%, which are extraordinarily high in comparison with other hausmannite occurrences (Ashley, 1989; Huebner *et al.*, 1992). Major element whole-nodule composition is characterized by high Mn_2O_3 contents (around 60%), significant
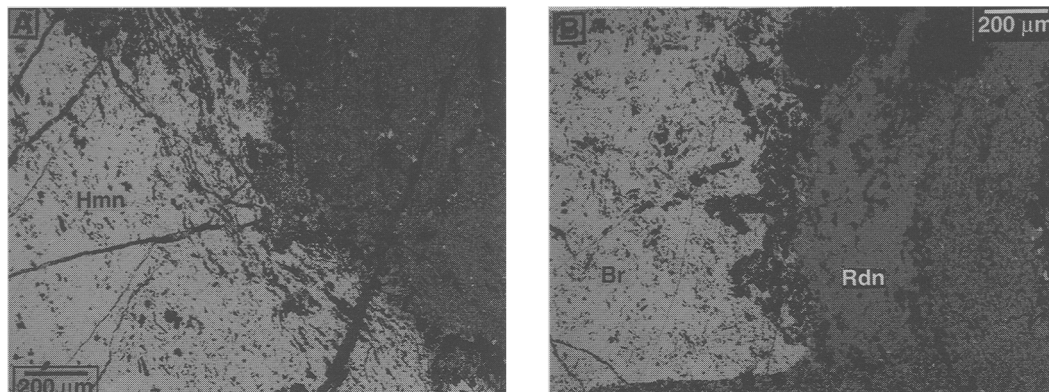
FIG. 1. (A) Backscattered electron image of tephroite band (Te) in contact with a hausmannite nodule (Hmn). (B) Backscattered electron image of rhodonite band (Rdn) in contact with a braunite nodule (Br).

Fe_2O_3 contents (around 10%) and low values of SiO_2, Al_2O_3, CaO, MgO, Na_2O and K_2O (Table 2). Notably Mn/Fe ratios are always high, showing values around 15. Regarding minor element contents, the most significant fact is the high values of chalcophile elements such as As, Sb and Zn. However, Cu, Ni, Co and rare earth element (REE) contents are extremely low. The REE patterns normalized to REE concentrations in European shale composite (Haskin and Haskin, 1966) show a slight enrichment

TABLE 1. Representative electron probe analyses of hausmannite

	1	2	3	4	5	6
SiO_2	1.02	0.11	1.70	0.23	0.15	0.14
TiO_2	0.24	0.22	0.17	0.05	0.07	0.12
Al_2O_3	0.91	0.58	0.69	0.50	0.62	0.54
Fe_2O_3*	5.35	7.30	5.05	6.20	5.61	5.84
Mn_2O_3*	94.72	94.29	95.56	95.72	94.54	94.81
MgO	0.06	0.02	0.06	0.05	0.04	0.03
CaO	0.14	0.03	0.08	0.02	0.03	0.04
Total	102.44	102.55	103.31	102.77	101.06	101.52
Si	0.039	0.004	0.064	0.009	0.006	0.005
Ti	0.007	0.006	0.005	0.001	0.002	0.003
Al	0.041	0.026	0.031	0.023	0.028	0.025
Fe^{3+}	0.154	0.212	0.144	0.178	0.164	0.170
Mn^{3+}	1.714	1.742	1.687	1.779	1.792	1.787
Mn^{2+}	1.037	1.008	1.063	1.006	1.004	1.006
Mg	0.003	0.001	0.003	0.003	0.003	0.002
Ca	0.005	0.001	0.003	0.001	0.001	0.002
Hausmannite	91.8	89.2	92.2	90.9	91.6	91.3
Jacobsite	8.2	10.8	7.8	9.1	8.4	8.7

Structural formulae normalized to 3 cations. Total Fe considered as Fe^{3+}.
Mn^{2+} and Mn^{3+} calculated by charge balance.
*Total Fe expressed as Fe_2O_3 and total Mn as Mn_2O_3.

of heavy *REE* in comparison to light *REE* (Fig. 2). In addition, hausmannite nodules display a characteristic negative Ce anomaly.

Braunite occurs as centrimetre-sized massive nodules, also without internal structure, included in a calcite matrix containing piemontite bands, albite, Mn-tremolite, spessartine, rhodonite, Mn-phlogopite, and Mn-diopside. The contact between the braunite nodules and the calcite matrix is characterized by the presence of rhodonite (Fig. 1B). Braunite micro-analyses (Table 3) show a composition close to ideal braunite I. Thus, Fe contents are extraordinarily low (<0.25 atoms p.f.u.). The most significant substitution is Mn^{2+} = Ca, which reach up to 0.26 atoms p.f.u. of Ca. Ostwald (1992) described metamorphic Ca-bearing braunite from the Mary Valley Manganese Belt (Australia). Whole-nodule composition shows that braunite nodules are very Mn-rich (around 55% of Mn_2O_3) and poorer in Fe than hausmannite nodules (less than 2 % of Fe_2O_3), which produces higher Mn/Fe ratios (around 35). Relatively high Ca contents (up to 10%) are due to the presence of calcite in the analysed powders. Trace-element composition of the braunite, as well as the hausmannite nodules, is characterized by high values of As and Sb, and low Co, Ni and Cu contents. Braunite *REE* concentrations are lower than those of the hausmannite nodules and the shale-normalized patterns do not show heavy *REE* enrichment in comparison with light *REE*. Moreover, the Aracena braunite-nodules do not show the Ce negative anomaly characteristic of the hausmannite nodules but show a weak Ce positive anomaly.

Origin

The Mn-rocks from the Aracena area are associated with jaspers, metabasites and metatuffs. Moreover, the Aracena Massif is characterized by numerous Cu sulfide ores associated with these rocks. In fact, the most important Cu sulfide deposit in this area (the Mina María Luisa) is located 300 m south of the outcrop studied here. These associations could be related with an exhalative volcanic submarine depositional environment (see Moorby *et al.*, 1984). The composition of hausmannite and braunite nodules is consistent with an exhalative submarine source for the formation of their precursors. Thus, the high Mn/Fe ratios, the anomalously high As and Sb values and the low *REE*, Co, Ni and Cu contents agree with the features of hydrothermal exhalative manganese deposits at submarine spreading centres and island arcs. Present day hydrothermal fluids from the ocean-floor spreading centres segregate Fe from Mn, and precipitate buserite that alters to birnessite, which could have been the precursors of the

TABLE 2. Selected whole-nodule compositions

	1	2	3	4
SiO_2	11.4	10.35	9.8	10.92
Al_2O_3	3.11	2.84	6.33	3.78
CaO	10.3	9.45	2.94	2.41
MgO	1.21	0.78	1.51	0.81
Na_2O	0.44	0.22	0.23	0.23
K_2O	0.41	0.56	0.52	0.22
Fe_2O_3*	1.76	1.82	10.53	9.35
Mn_2O_3*	54.85	55.94	62.62	63.63
TiO_2	0.09	0.08	0.27	0.25
P_2O_5	0.03	0.02	0.03	0.02
As	620	754	4610	4278
Sb	200	215	1320	1209
Zn	64.4	70	215	192
Ba	160	200	2314	2613
Co	4	4	6	6.5
Ni	36	14	21	18.6
Cu	9.7	9.5	3.1	3.8
V	13	11	12	12.1
La	12.7	13.2	33.5	30.4
Ce	30.1	30.4	26.1	27.6
Nd	8.8	9.2	24.9	26.9
Sm	1.7	1.9	4.4	3.4
Eu	0.3	0.5	0.9	1
Tb	0		1.7	0
Yb	1	1	5	4.1
Lu	0.2	0.2	0.7	0.6

1 and 2: Braunite nodules. 3 and 4: Hausmannite nodules.
Major elements as oxide weight per cent and minor elements as ppm.
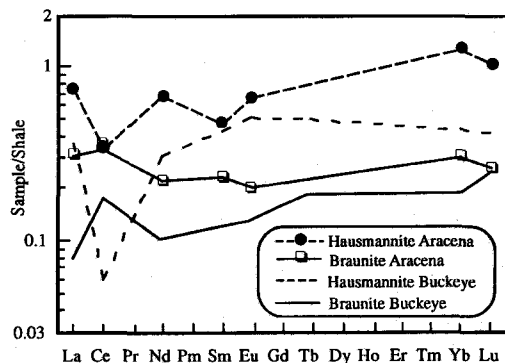*Total Fe expressed as Fe_2O_3 and total Mn as Mn_2O_3.

FIG. 2. *REE* patterns of hausmannite and braunite nodules normalized to *REE* concentrations in the European shale composite (Haskin and Haskin, 1966). For comparison, data of Buckeye Mine from Huebner *et al.* (1992).

TABLE 3. Representative electron probe analyses of braunite

	1	2	3	4
SiO_2	10.37	11.77	11.39	11.43
TiO_2	0.01	0.05	0.00	0.05
Al_2O_3	0.99	1.91	0.87	2.13
Fe_2O_3*	0.20	3.45	0.17	2.56
Mn_2O_3*	88.28	81.54	86.12	81.50
MgO	0.02	0.10	0.05	0.20
CaO	1.15	1.74	2.45	1.92
Total	101.02	100.56	101.05	99.79
Si	1.036	1.168	1.129	1.140
Ti	0.000	0.004	0.000	0.004
Al	0.116	0.223	0.101	0.250
Fe^{3+}	0.015	0.257	0.013	0.192
Mn^{3+}	5.800	5.182	5.634	5.272
Mn^{2+}	0.907	0.966	0.856	0.908
Mg	0.003	0.015	0.007	0.029
Ca	0.123	0.185	0.260	0.205

Structural formulae normalized to 8 cations. Total Fe considered as Fe^{3+}.
Mn^{2+} and Mn^{3+} calculated by charge balance.
*Total Fe expressed as Fe_2O_3 and total Mn as Mn_2O_3.

metamorphic braunite and hausmannite nodules in the Aracena area. However, the variations of the Ce anomaly can be related with the evolution of hydrothermal fluids. Unlike other *REE*, Ce speciation can change from dissolved Ce^{3+} complexes in reducing, acid Mn-transporting hydrothermal fluids to form CeO_2 from oxidized, alkaline waters. Crystallization of braunite indicates more oxidizing conditions than for hausmannite, as the Mn^{3+}/Mn^{2+} ratio of the former is 6:1, whereas that of hausmannite is 2:1. The presence of a pronounced Ce negative anomaly in the hausmannite nodules is consistent with precipitation under more reducing conditions than those of the braunite nodules, which lack a Ce negative anomaly. This would indicate the relative proportion of hydrothermal fluid and seawater from which the Mn-oxides were precipitated. Thus, the braunite precursor could be precipitated from fluids richer in seawater than those from which the hausmannite precursor was precipitated. Huebner *et al.* (1992) observed a similar relation between the hausmannite and braunite protoliths from the Buckeye deposit (California).

In conclusion, the chemical signature of the hausmannite and braunite nodules from the Aracena area, as well as the association of the nodules with jaspers, metabasites and Cu-deposits are consistent with the formation of the deposit as a submarine hydrothermal system, probably in a rifting environment. The presence of hausmannite and braunite nodules can be considered as a consequence of the evolution of the hydrothermal fluids when mixed with varying amounts of seawater.

Metamorphism

On the basis of the microscopic data two metamorphic stages can be deduced from the studied rocks: 1) Hausmannite and braunite may well represent metamorphic transformations of their hydrothermal precursors formed during regional metamorphism to greenschist facies. However, braunite could have been produced during diagenetic reactions between the manganese oxide and the silica present in the sediments, and could be considered inert to the greenschist-facies metamorphism. During this stage, spessartine garnet crystallized in the matrix containing hausmannite nodules, whereas piemontite formed in a carbonate matrix containing the braunite nodules. 2) The intrusion of the nearby dioritic body caused a contact metamorphic stage, which produced the crystallization of tephroite at the contact with the hausmannite nodules, and the formation of rhodonite at the contact with the braunite nodules. Textural and chemical relations of minerals in both metamorphic stages are described in Jimenez-Millán and Velilla (1993, 1994). The formation of spessartine suggests a lower temperature limit around 400°C (Hsu, 1968). The presence of titanite in the carbonate rocks containing braunite nodules allows us to constrain the upper temperature limit by the titanite disappearance curve (Moody *et al.*, 1983), which indicates temperatures lower than 500°C. It is interesting to note that Flohr (1992) suggested that preservation of the trace-element signatures indicative of submarine hydrothermal processes can survive amphibolite-facies metamorphism.

Acknowledgements

References

Ashley, P.M. (1989) *Neues Jahrb. Mineral. Abh.*, **161**, 85–111.
de Villiers, J.P.R. (1975) *Amer. Mineral.*, **60**, 1098–104.
de Villiers, J.P.R. and Herbstein, F.H. (1967) *Amer.*

Mineral., **52**, 20.

Flohr, M.J.K. (1992) *Econ. Geol.*, **87**, 2023–40.

Haskin, M.A. and Haskin, L.A. (1966) *Science*, **154**, 507.

Huebner, J.S. (1976) The manganese oxides: A bibliographic commentary. In: *Mineral. Soc. Amer. Reviews in Mineralogy*, **5**, SH1–17.

Huebner, J.S., Flohr, M.J.K. and Grossman, J.N. (1992) *Chem. Geol.*, **100**, 93–118.

Hsu, L.C. (1968) *J. Petrol.*, **9**, 40–83.

Jiménez-Millán, J. and Velilla, N. (1993) *Eur. J. Mineral.*, **5**, 961–70.

Jiménez-Millán, J. and Velilla, N. (1994) *Neues Jahrb.*

Mineral. Abh., **166**, 193–209.

Moody, J.B., Meyer, D. and Jenkins, J.E. (1983) *Amer. J. Sci.*, **283**, 48–92.

Moorby, S.A., Cronan, D.S. and Glasby (1984) *Geochim. Cosmochim. Acta*, **48**, 433–41.

Ostwald, J. (1992) *Mineral. Deposita*, **27**, 326–35.

Robie, R.A., Huebner, J.S. and Hemingway, B.S. (1995) *Amer. Mineral.*, **80**, 560–75.

Platinum-group minerals from the Nuasahi ultramafic-mafic complex, Orissa, India

Sisir K. Mondal*
Tapan K. Baidya

Department of Geological Sciences, Jadavpur University, Calcutta - 700 032, India

THE Precambrian ultramafic-mafic complex of Nuasahi (21°16′N, 86°20′E), Orissa, in the Eastern Indian Shield is reported to contain economically significant amounts of the platinum-group elements (PGE), with Au and Ag in an Fe-Cu-Ni-Co-sulphide mineralized brecciated zone at the interface of the chromiferous ultramafites and gabbro. This is the first reported occurrence of four platinum-group minerals (PGM), sudburyite, michenerite, palladian-bismuthian melonite and irarsite from the chromite-sulphide assemblage of this sulphide mineralized area. The elongated north–south trending ultramafic and mafic rocks are emplaced within the metasediments and metavolcanics of the Iron Ore Group (3200 Ma, Saha *et al.*, 1988). A more or less stratiform sequence from ultramafic to mafic, olivine-websterite, dunite, harzburgite, chromitite,

* Present address: Refractory Research Division, Central Glass & Ceramic Research Institute (C.S.I.R.), 196, Raja S.C. Mullick Rd., P.O. Jadavpur University, Calcutta-700032, India.

orthopyroxenite, norite, gabbro, anorthosite and titaniferous magnetite is preserved with a general north–south trend and easterly dip. Three chromitite horizons, the Durga lode, the Laxmi lode (Laxmi-2 and Laxmi-1) and the Shankar lode (from west to east) are being mined for chrome ores.

Sulphide mineralization and chromite-sulphide assemblage

The easternmost chromiferous horizon, i.e the Shankar lode, is highly disrupted with the formation of the northerly trending brecciated zone (7–15 m wide) extending over a length of 1 km along the strike and impregnated by the gabbro-noritic rock at the hanging-wall side. This zone is a heterogenous assemblage of differently oriented angular to subrounded blocks/fragments of massive, spotted and banded chromitite, serpentinite, coarse-grained pyroxenite, some hybrid rocks which are pervaded by the leucogabbro, dolerite and clinopyroxenite. Enrichment of sulphide is found in the matrix material of this zone with disseminated chromite